1 MATCHING HALOS

In this section, we ran a set of convergence tests using small simulation boxes.

1.1 Mass Resolution

1.2 Step Size

1.2.1 Algorithm

Here, we investigated how the number of step sizes affect on halo properties (i.e., halo mass, position, and velocity) and statistical observables. The mass resolution is fixed to 256^3 particles in the cubical box of $(256h^{-1}\mathrm{Mpc})^3$.

Since our simulations all start with the same initial conditions, we match halos in different simulations by matching their particle content. Given a halo in simulation A, we consider the halos in simulation B that its particles correspond to. Given this list of possible matches, we match to the halo with the largest number of common particles. To avoid spurious matches, we also require that this fraction of common particles (relative to simulation A) exceeds a chosen threshold. Figure 1 Shows the cumulative fraction of unmatched halos matching the 450/5 to the 300/2 simulation at $z = 0.15$ with various thresholds. As expected, the unmatched fraction increases with increasing threshold and decreasing hao mass. We adopt a threshold of 50% as out default choice.

Since the above matching algorithm is unidirectional, multiple halos in A might be matched to a single halo in B; this happens 1 to 2% of the time with a matching threshold of 50%. We refer to these as multiply-booked halos in what follows. Figure 2 compares halo mass for the matched halos between the 450/5 and the 300/2 simulations at $z = 0.15$. We classified those matched halos into multiply-booked halos and the rest. As shown in Figure 2, the summed halo mass for those multiply-booked halos in the 450/5 is correlated with the corresponding halos in the 300/2 better than the individual halo mass in the 450/5. This inplies that those multiply-booked halos in the 450/5 are merged into one halo in the 300/2. Since larger global steps and sub-cycles can capture dynamics better, it is likely that the halos in the 450/5 forms sub-structure ealier than the 300/2 simulation.

Figure 3 shows the number densities of the unmatched halos in the 450/5 matching to the 300/2 at $z = 0.15$. There are three reasons that halos are considered as unmatched. First, if there

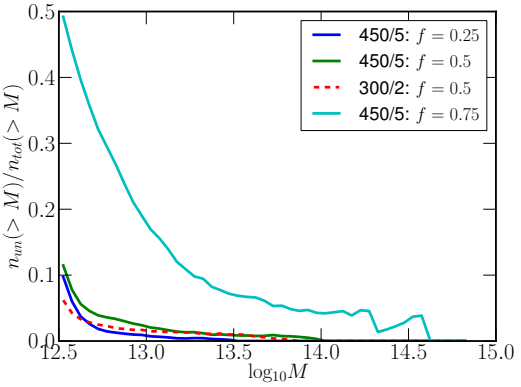

Figure 1. The cumulative fraction of unmatched halos matching the 450/5 to the 300/2 simulation at z=0.15 as a function of halo mass. The solid lines, from top to bottom, correspond to matching thresholds of 75%, 50%, and 25%. The dashed line shows the same quantity except now matching the 300/2 to the 450/5 simulation for a threshold of 50%. As expected, the unmatched fraction increases with decreasing halo mass and increasing threshold. We adopt a threshold of 50% as our default choice.

are no common particles in the halos, we consider them as unmatched. Second, if the fraction of common particles over the total number of particles in each halo is less than 50%, we eliminate those spurious halos. At last, we remove the multiply-booked halos except the ones which have the most number of common particles. We showed each unmatched number density as a function of halo mass. There are only low-mass unmatched halos for not having any common particles. This is because low-mass halos are formed with smaller number of particles and it is likely that particles in a halo in A do not form a halo in B. As shown, most of unmatched halos are due to the threshold criterion.

In Figure 4, we show the cumulative fractions of unmatched halos as a function of redshift and the number of step size. As shown in the right panel in Figure 4, the fractions are almost the same for different redshifts. On the other hand, the left panel in Figure 4 shows that global time steps actually affect to the fraction of unmatched halos on any halo mass and sub-cycles make differences on low-mass halos.

1.2.2 Halo Properties

Here, we present halo properties (i.e., halo mass, position, and velocity) for matched halos match-

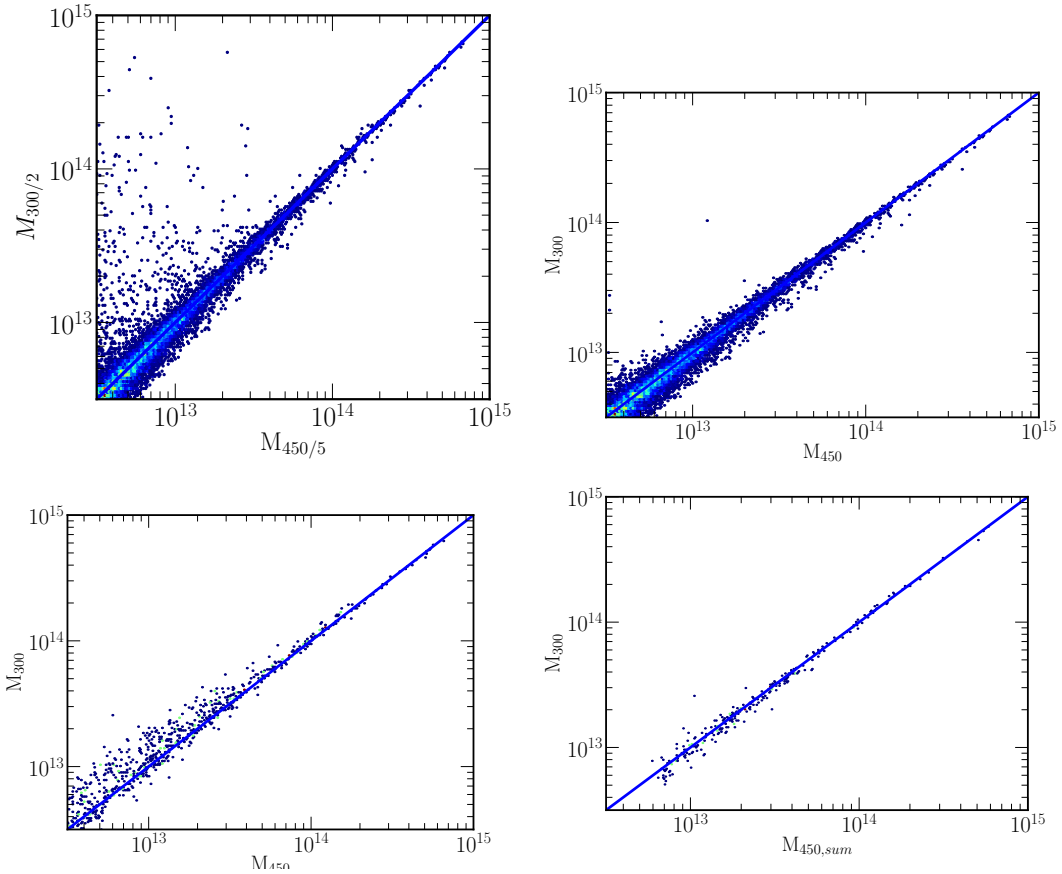

Figure 2. (Change the shape of the plots)The comparison of halo mass for the matched halos matching the 450/5 to the 300/2 simulation at $z = 0.15$. The x-axis is the halo masses for the 450/5 simulation and the y-axis is the halo masses for the 300/2 simulation. The top left panel shows the mass scatter of all the matched halos. As shown, there are some matched halos in the 300/2, which are more massive than the halos in the 450/5. The top right panel compares for halos which are not "multiply-booked halos". This plot does not show the positive mass discrepancy between the 300/2 and the 450/5 simulations. The bottom panels are for "multiply-booked halos". While we plotted all the "multiply-booked halos" in the left panel, we summed halo masses of the "multiply-booked halos" in the right panel. Those plots indicate that those "multiply-booked halos" in the 450/5 are merged into one halo in the 300/2.

ing to the 450/5, taken as a reference. The panels in Figure 5, from left to right, show the comparison of halo mass, position, and velocity for the matched halos at $z = 0.15$. As shown, the 150 global steps have more scatter in the halo properties and the means are off from the center to the halo mass ratio and the velocity difference. This indicates that the halo structure in these cases is more diffused than the case of the 300 or the 450 global steps. For the 300 global steps, the results are siginificantly improved and the center position is matched in these cases to better than 200 kpc. As is clear from Figure 5, the difference between 3 and 2 sub-cycles is negligible on halo properties. The same results shown in Figure 5 but for other redshifts are in Table 1, 2,3, and 4, and they support the same argument discussed for Figure 5. Table 4 shows fractions of halos whose velocity directions are matched to the ones for the 450/5 within 10 degree. More than 90% of the matched halos have angles between the velocities within 10 degree at all the redshifts, $z = 0.15$, $z = 0.5$, and $z = 0.8$.

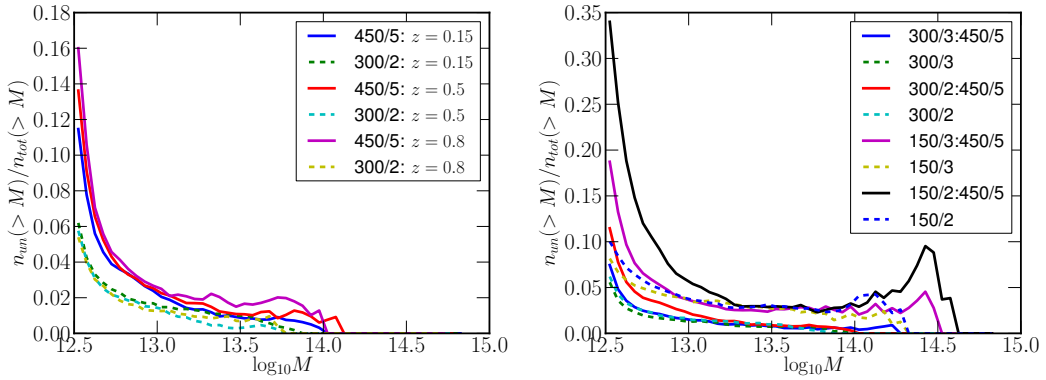

[p]

Figure 4. Right: (Remove dashed lines) The cumulative fraction of unmatched halos matching the 450/5 to the 300/2 as a function of redshift. The plot shows that the unmatched fraction does not depend on redshift. Left: The cumulative fraction of unmatched halos matching the 450/5 to the other step sizes at $z = 0.15$. As shown, sub-cycles only affect on low-mass end. All the sample are 256^3 particle simulations.

[t]

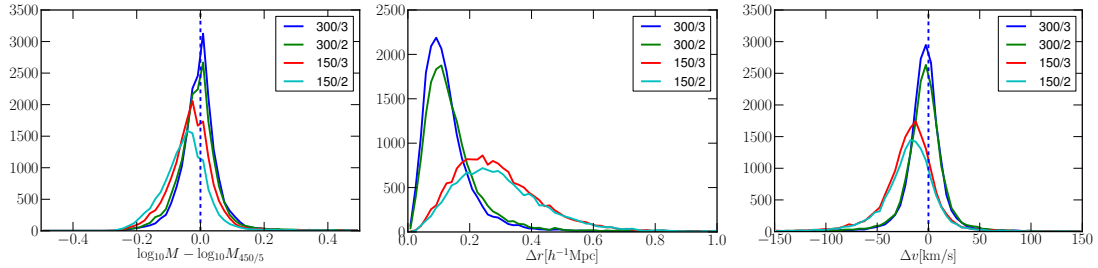

Figure 5. Comparison of halo properties (i.e., halo mass, position, and velocity) for matched halos matching to the 450/5 simulation, taken as a reference, at $z = 0.15$. Left: (Change x-axis and its label) Comparison of halo masses as a histogram of halo mass ratio to the 450/5. Different colors correspond to different number of step size: 300/3 (blue), 300/2 (green), 150/3 (red), and 150/2 (light blue). As shown, the means for the 150 global steps simulation are slightly off from the center and sub-cycles are less effective on halo mass. Middle: Comparison of halo position as a histogram of distance between the matched halos matching to the 450/5. Color scheme used here is the same as for halo mass. The plot shows more scatter for the case of the 150 glbal steps to the center position. For the 300 global time steps, the results improve considerably, and the center position is matched in these cases to better than 200 kpc. Right: Comparison of velocity as a histogram of velocity difference in magnitude between the matched halos to the 450/5. Color scheme used here is the same as the plots of halo mass and position. As clearly shown, the means for the 150 global steps are negatively(?) off from the center and the velocity differences to the 450/5 are more scattered. It implies that halo structures in the 150 global steps are more diffuse than the structure in the 450/5 and they have shallower potential well. All the comparisons indicate that the difference between 3 and 2 sub-cycles in this case is negligible.

1.2.3 Quantitative Tests

Here, we show several quantitative tests including comparison of mass functions and cross power spectra as a function of time steps, redshift, and halo mass. Since the 300/2 simulation is our final target, we mainly focus on the comparison between the 450/5 and the 300/2 simulations.

In Figure 6, we caluculated mass functions for the simulations with 256^3 particles as a function of time steps and compared them to the simulation with 512^3 particles at $z = 0.15$. For the simulation of 512^3 particles, the number of time step used here is always 450/5. As shown, mass functions for the 450 and the 300 global steps with 256^3 particles match to the 512^3 particles simulation better than10 percent and the effect of 3 and 2 sub-cycles for the 300 global steps

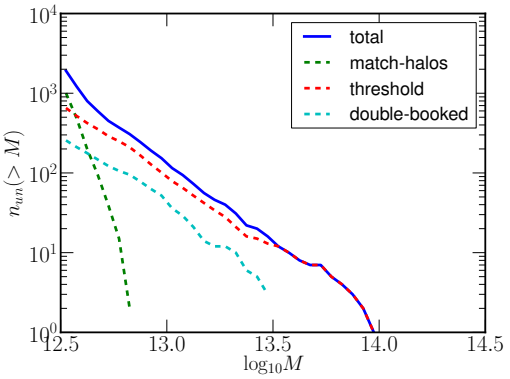

Figure 3. (Change the legends) The number density of unmatched halos in the 450/5 simulation matching to the 300/2 as a function of halo mass at $z = 0.15$. The solid line represents the total number density of unmatched halos with a threshold of 50%. The dashed lines are the number densities of the unmatched halos based on different criteria. The unmatched density shown as the green line is due to not finding any common particle in the 300/2 simulation. The red line is due to the threshold of 50% as the fraction of common particles over the total number of particles in each halo in the 450/5. The light blue line is due to eliminating multiply-booked halos except the ones which have the most common particles. As shown, most of unmatched halos are due to the threshold of 50%.

are mainly on low-mass halos. This supports the choice of the 300/2 as our final choice. In Figure 7, we compare the 300/2 to the 450/5 as a function of redshift. In the left panel of Figure 7, we calculated the errors for the mass functions of 512^3 particles through the bootstrap method and compared the mass functions for the 300/2 and the 450/5 simulation with 256^3 particles to the 512^3 particles simulations at $z = 0.15$ and $z = 0.8$. Those mass functions for 256^3 particles are well within the errors for the 512^3 particles simulations. In the right panel of Figure 9, we compared the mass functions for the 300/2 to the 450/5 as a function of redshift. As shown, the agreement between the 300/2 and the 450/5 decreases as decreasing halo mass and increasing redshift, but all the mass functions for the 300/2 match to the 450/5 at 5 per cent on the mass range from $10^{13}M_\odot$ to $10^{14}M_\odot$. One possible explanation for decreasing number densities for the 300/2 on low-mass halos is that halos in the 300/2 tend to be more puffed up than the ones in the 450/5 due to small number of short-range time steps and some particle clustering in the 300/2 are not defined as halos by FOF.

In order to study how the fluctuation (difference?) of position shown in Figure 5 affects on halo bias, we calculated halo-matter cross power spectra shown in Figure 8, Figure 9, and Figure 10. Here, we used the dark matter density field of the 450/5 simulation with 256^3 particles for all the cross power spectra. The comparison of halo-matter cross power spectra gives an idea about halo bias. In Figure 8, we compared the cross power spectra for various time steps to the 450/5 at $z = 0.15$. The halo biases for the 300 global steps match to the halo bias for the 450/5 at 5 per cent, while the biases for the 150 global steps gets larger on small scales. We compared the cross power spectra for the 300/2 to the 450/5 as a function of redshift and halo mass slices in Figure 9 and Figure 10 respectively. As shown, the halo bias for the 300/2 gets larger as increasing redshift. On the other hand, selection of halo mass seems to give no effect on the halo bias.

To investigate the effect of variation on velocity shown in Figure 5, we calculated halo auto power spectra in redshift-space in Figure **??** and Figure **??** as a function of time step and redshift. As shown in Figure **??**, the monopole terms of the redshift-space auto power spectra for the 300 global steps match to the 450/5 at 5 per cent and the sub-cycles gives negligible effect on those monopoles. We also compared the monopoles for the 300/2 to the 450/5 as a function of redshift, shown in Figure **??**. We did not see siginificant effect of redshift on those monopoles.

As the last quantitative test, we computed galaxy-matter cross power spectra for the 300/2 and the 450/5 through Halo Occupation Distiributions (HODs). The HOD gives a conditional probability for the number of central and satellite galaxies in a halo and populates halos with galaxies based on a set of parameters and halo mass. Here, we used the formulation proposed by Zheng et al. 2005:

$$< N_{cen} >= \frac{1}{2}[1 + erf(\frac{\log M_{cut} - \log M_{halo}}{\sqrt{2}\sigma})]$$

$$< N_{sat} >=< N_{cen} > (\frac{M_{halo} - \kappa M_{cut}}{M_1})^\alpha,$$

where M_{cut},σ,κ,M_1, and α are set of free parameters. We set the parameters to $M_{cut} = 13.06$,$M_1 = 14.0$,$\sigma = 0.21$,$\kappa = 1.5$, and $\alpha = 1.19$ in Figure **??**. As shown, the trend shown in the halo-matter cross power spectra, which is the in-

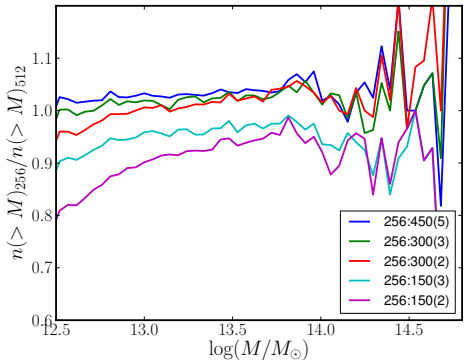

Figure 6. Comparison of mass functions for the simulations with 256^3 particles as a function of time step at $z = 0.15$, using the simulation with 512^3 particles as a reference. Different colors correspond to different number of time steps. As shown, the mass functions for the 450 and the 300 global steps match to the simulation of 512^3 particles at 10 percent, except on high-mass end where there are a fewer number of halos.

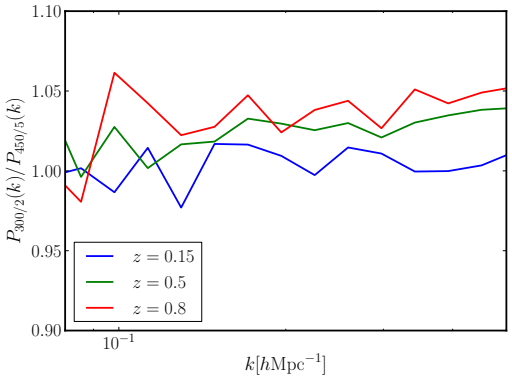

Figure 9. Comparison of halo bias between the 450/5 and the 300/2 simulations by comparing halo-matter cross power spectra as a function of redshift. Different colors correspond to different redshifts, as labeled in the figure. The mass threshold used here is $10^{12.5}\mathrm{M}_\odot$. The cross power spectra for the 300/2 match to the 450/5 at almost 5 per cent for all the redshifts. As shown, the deviation from the 450/5 gets larger as increasing redshift.

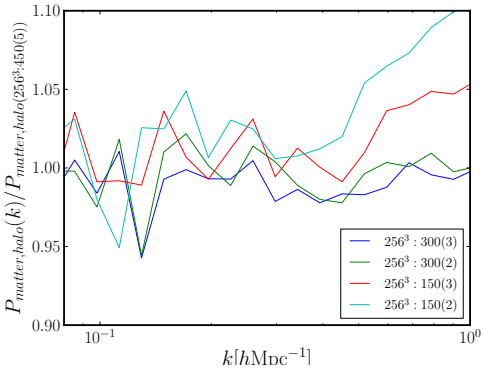

Figure 8. Comparison of halo bias for various time steps to the 450/5 by comparing halo-matter cross power spectra at $z = 0.15$. The mass range for halos used here is from $10^{12.5}\mathrm{M}_\odot$ to $10^{13}\mathrm{M}_\odot$. Different colors correspond to different number of time steps, as labeled in the figure. The cross power spectra for the 300 global steps match to the 450/5 at 5 per cent on any scales, while the halo bias for the 15o global steps becomes larger on small scales.

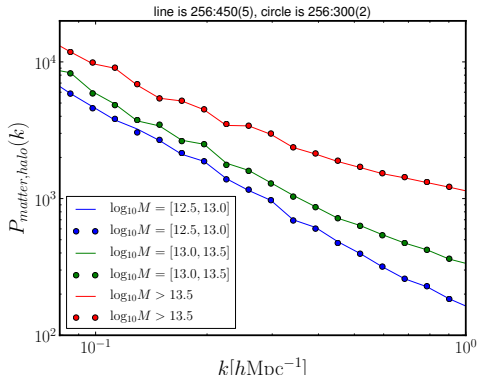

Figure 10. Comparison of halo bias between the 450/5 and the 300/2 simulations by comparing halo-matter cross power spectra as a function of mass slices at $z = 0.15$. Different colors correspond to different mass slices as labeled in the figure. The solid lines represent the cross power spectra for the 450/5 and the circle lines are for the 300/2. For any halo mass slices, the cross power spectra for the 300/2 match sufficiently to the 450/5.

crease of bias for the 300/2 to the 450/5 as increasing redshift, in Figure 9 is somewhat supressed and all the cross power spectra for the 300/2 match to the 450/5 at almost 2 per cent, but note that this agreement depends on the choice of the HOD parameters.

[h] Table: $\log_{10}(M/M_{450/5})$

z=0.15	median	$\Delta_{95\%}$	$\Delta_{65\%}$
300/3	-0.0026	0.2864	0.0877
300/2	-0.0078	0.3458	0.0972
150/3	-0.0266	0.3101	0.1107
150/2	-0.0454	0.3315	0.1207

z=0.5	median	$\Delta_{95\%}$	$\Delta_{65\%}$
300/3	-0.0062	0.2869	0.0905
300/2	-0.0139	0.3345	0.1029
150/3	-0.0372	0.3083	0.1148
150/2	-0.0595	0.3093	0.1252

z=0.8	median	$\Delta_{95\%}$	$\Delta_{65\%}$
300/3	-0.0067	0.2891	0.0932
300/2	-0.0189	0.3347	0.1048
150/3	-0.0519	0.2926	0.1172
150/2	-0.0782	0.28878	0.1274

Table 1. Comparison of halo mass ratios $\log_{10}M/M_{450/5}$ in log-based, comparing various time steps to the 450/5 simulation at $z = 0.15$, $z = 0.5$, and $z = 0.8$. For each redshift, we report median, $\Delta_{95\%}$, and $\Delta_{65\%}$ (how should I explain about $\Delta_{95\%}$?). As shown in Figure 5, the results indicate that mass ratio distributions for the 300 global steps have less scatter than for the 150 global steps.

[H]

z=0.15	median	$\Delta_{95\%}$	$\Delta_{65\%}$
$M_{halo} \in [10^{12.5}, 10^{13.0}]$	-0.0111	0.3896	0.1124
$M_{halo} \in [10^{13.0}, 10^{13.5}]$	-0.0085	0.2599	0.0748
$M_{halo} \in [10^{13.5}, 10^{14.0}]$	-0.0056	0.1596	0.0471
$M_{halo} > 10^{14.0}$	-0.0047	0.1323	0.0341

z=0.5	median	$\Delta_{95\%}$	$\Delta_{65\%}$
$M_{halo} \in [10^{12.5}, 10^{13.0}]$	-0.0197	0.3544	0.1156
$M_{halo} \in [10^{13.0}, 10^{13.5}]$	-0.0123	0.2546	0.0790
$M_{halo} \in [10^{13.5}, 10^{14.0}]$	-0.0067	0.1813	0.0497
$M_{halo} > 10^{14.0}$	-0.0052	0.0731	0.0309

z=0.8	median	$\Delta_{95\%}$	$\Delta_{65\%}$
$M_{halo} \in [10^{12.5}, 10^{13.0}]$	-0.0260	0.3478	0.1161
$M_{halo} \in [10^{13.0}, 10^{13.5}]$	-0.0167	0.2546	0.0835
$M_{halo} \in [10^{13.5}, 10^{14.0}]$	-0.0084	0.1809	0.0490
$M_{halo} > 10^{14.0}$	-0.0077	0.1361	0.0297

Table 2. Comparison of halo mass ratios $\log_{10}M_{300/2}/M_{450/5}$ in log-based, comparing the 300/2 to the 450/5 simulation as a function of halo mass slices at $z = 0.15$, $z = 0.5$, and $z = 0.8$. For each redshift, we report median, $\Delta_{95\%}$, and $\Delta_{65\%}$. As shown, medians and Δs decreases as increasing halo mass and decreasing redshift.

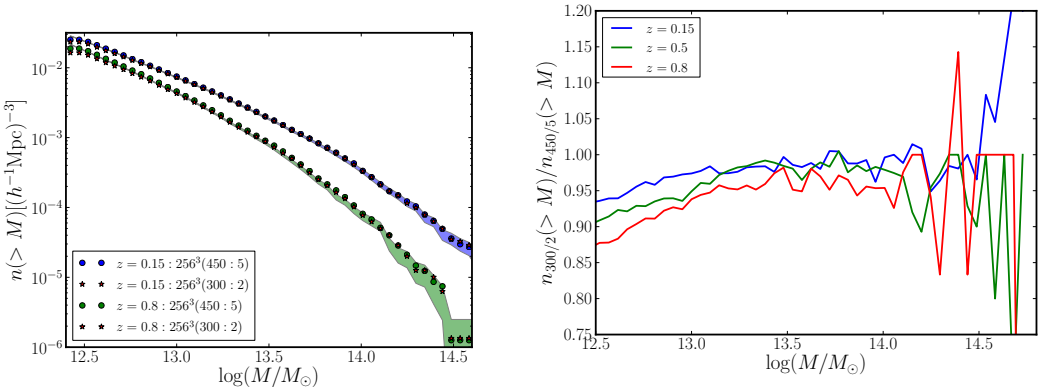

Figure 7. Left: Comparison of the halo number densities for the 300/2 and the 450/5 simulation with 256^3 particles to the simulation with 512^3 particles at $z = 0.15$ and $z = 0.8$. The shaded regions are the number densities for the 512^3 particles samples, including errors calculated from the bootstrap method. The circle line is for the 450/5 and the star line is for the 300/2 with 256^3 particles. The number densities from top to bottom correspond to $z = 0.15$ and $z = 0.8$ respectively. Both the number densities for the 450/5 and the 300/2 are within the errors (?) for the 512^3 particles. Right: The ratio of the number densities of the 300/2 to the 450/5, which have the same mass resolution, as a function of redshift. The 300/2 matches to the 450/5 at 10 per cent on the mass range from $10^{13}\mathrm{M}_\odot$ to $10^{14}\mathrm{M}_\odot$. As indicated, the agreement (?) between the 450/5 and the 300/2 decreses with increasing redshift on low-mass end.

[H]

z=0.15	median	$\Delta_{95\%}$	$\Delta_{65\%}$
300/3	0.1116	0.4439	0.1228
300/2	0.1245	0.5558	0.1406
150/3	0.2706	0.6234	0.2571
150/2	0.2800	0.6568	0.2680

z=0.5	median	$\Delta_{95\%}$	$\Delta_{65\%}$
300/3	0.1221	0.4700	0.1298
300/2	0.1348	0.5400	0.1460
150/3	0.2382	0.5555	0.2248
150/2	0.2475	0.5835	0.2335

z=0.8	median	$\Delta_{95\%}$	$\Delta_{65\%}$
300/3	0.1217	0.4553	0.1329
300/2	0.1354	0.4969	0.1498
150/3	0.2447	0.5408	0.2284
150/2	0.2536	0.5418	0.2334

Table 3. Comparison of halo positions for various time steps to the 450/5 simulation at $z = 0.15$, $z = 0.5$, and $z = 0.8$. For each redshift, we report median, $\Delta_{95\%}$, and $\Delta_{65\%}$. As shown, the halo positions for the 150 global steps are more scattered and 3 and 2 sub-cycles affect negligibly on halo positions. Also, there is little change due to redshift.

z=0.15	median	$\Delta_{95\%}$	$\Delta_{65\%}$
300/3	-3.36	82.20	24.3872
300/2	-3.26	99.40	27.5063
150/3	-16.61	116.93	38.4702
150/2	-17.05	121.45	39.9572

z=0.5	median	$\Delta_{95\%}$	$\Delta_{65\%}$
300/3	-3.78	118.48	36.87
300/2	-3.94	137.62	40.77
150/3	-23.25	151.75	53.41
150/2	-24.26	160.15	56.75

z=0.8	median	$\Delta_{95\%}$	$\Delta_{65\%}$
300/3	-6.32	149.72	47.41
300/2	-6.47	169.1556	53.48
150/3	-25.23	186.29	67.62
150/2	-24.76	189.26	71.97

Table 4. Comparison of halo velocity for various time steps to the 450/5 simulation at $z = 0.15$, $z = 0.5$, and $z = 0.8$. For each redshift, we report median, $\Delta_{95\%}$, and $\Delta_{65\%}$. As shown in Figure 5, the results indicate that mass ratio distributions for the 300 global steps have less scatter than for the 150 global steps.

z=0.15	fraction within 10 degree
300/3	0.951
300/2	0.938
150/3	0.928
150/2	0.923

Table 5. Fractions of halos whose velocity direction matches with the 450/5 within 10 degree at $z = 0.15$. More than 90% f halos for any time steps agree with the 450/5 simulation.